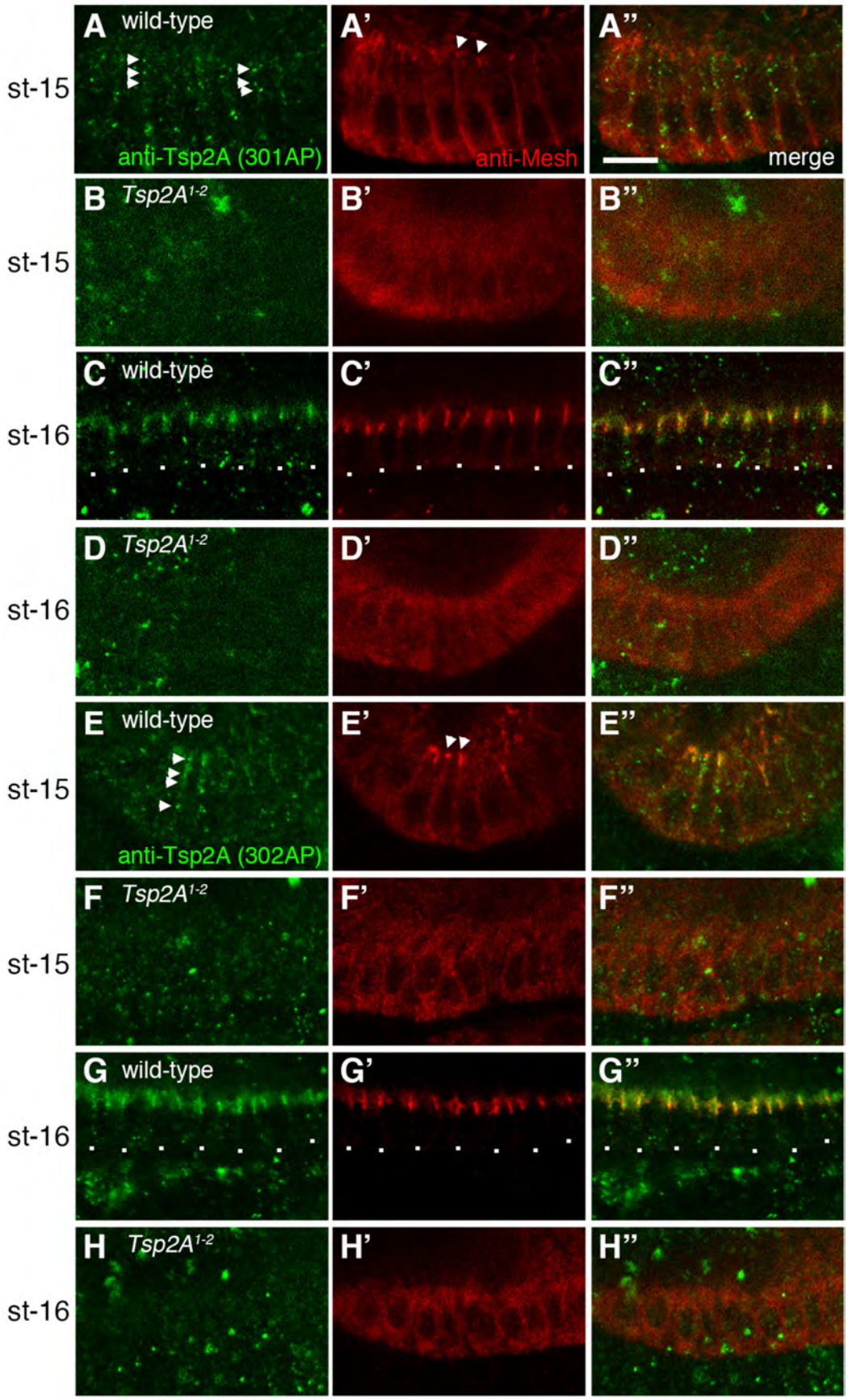

Figure S1. Tsp2A and Mesh distribution during sSJ formation in wild-type and *Tsp2A*$^{1-2}$-mutant embryos

(**A-H**”) Double-staining of stage-15 wild-type embryos (A-A” and E-E”), *Tsp2A*$^{1-2}$-mutant embryos (B-B” and F-F”), stage-16 wild-type embryos (C-C” and G-G”) and *Tsp2A*$^{1-2}$-mutant embryos (D-D” and H-H”) with a combination of anti-Tsp2A antibody (301AP for A-D or 302AP for E-H) and anti-Mesh antibody (A’-H’). Arrowheads in A and E indicate the aggregates of Tsp2A along the lateral membrane. Arrowheads in A’ and E’ indicate the apicolateral accumulation of Mesh. Scale bar: 5 μm (A-H”).

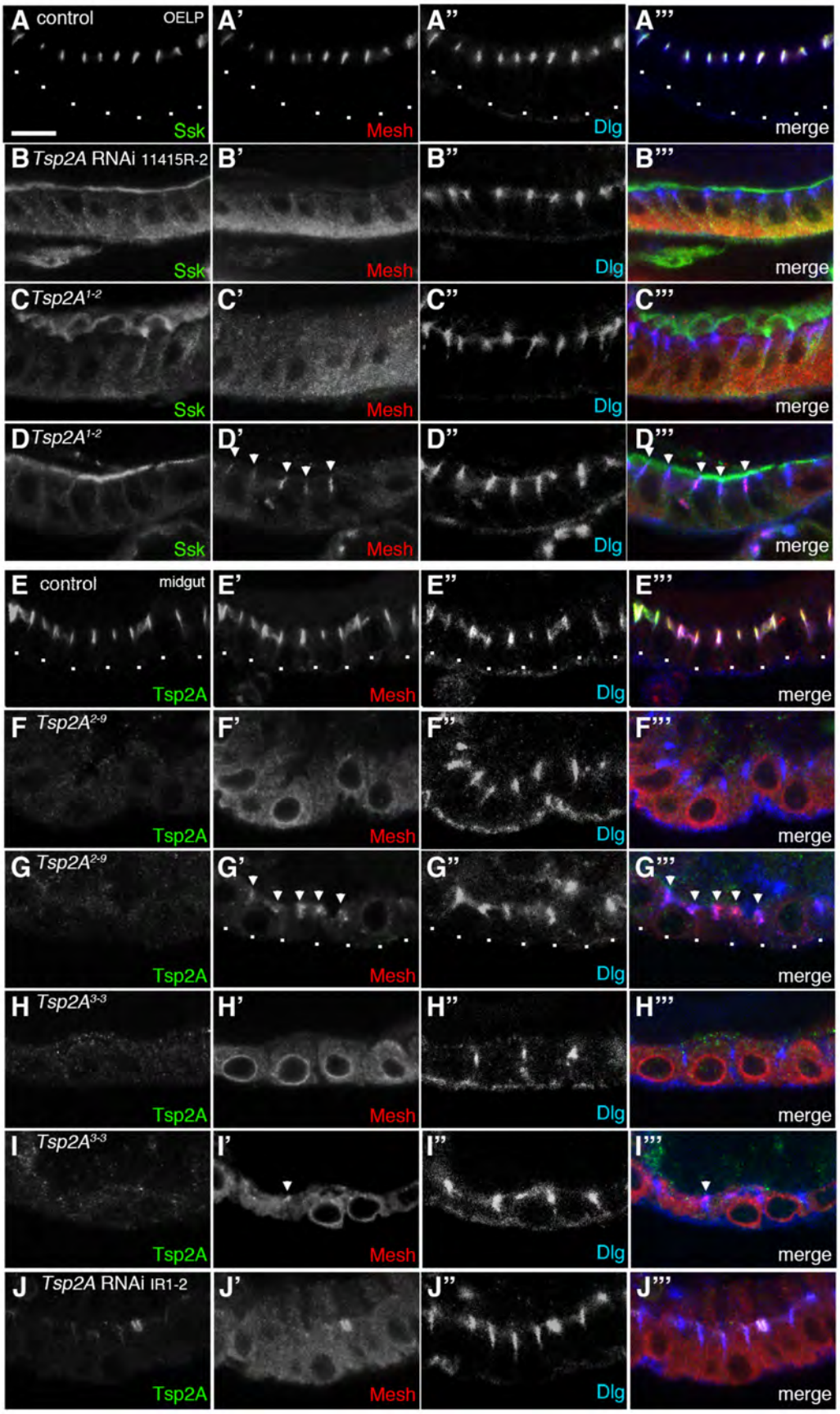

Journal of Cell Science • Supplementary information

Figure S2. sSJ components are mislocalized in *Tsp2A*-mutant epithelial cells.
(**A-D”’**) The first-instar larval OELP of control (A-A”’), *Tsp2A*-RNAi 11415R-2 (B-B”’) and $Tsp2A^{1-2}$-mutant (C-C”’ and D-D”’) stained with anti-Ssk (A-D), anti-Mesh (A’-D’) and anti-Dlg (A”-D”) antibodies. The merged images are shown in A”’-D”’, where the staining of anti-Ssk, anti-Mesh, and anti-Dlg is shown by green, red and blue, respectively. Arrowheads in D’ and D”’ indicate the apicolateral localization of Mesh in $Tsp2A^{1-2}$-mutant OELP.
(**E-J”’**) The first-instar larval midgut of control (E-E”’), $Tsp2A^{2-9}$ (F-F”’ and G-G”’), $Tsp2A^{3-3}$ (H-H”’ and I-I”’) mutants and *Tsp2A*-RNAi IR1-2 (J-J”’) stained with anti-Tsp2A (E-I), anti-Mesh (E’-I’) and anti-Dlg (E”-I”) antibodies. The merged images are shown in E”’-J”’. Arrowheads in G’, G”’, I’ and I”’ indicate the apicolateral localization of Mesh in $Tsp2A^{1-2}$-mutant epithelial cells. Basal membranes are delineated by dots. Scale bar: 5 µm.

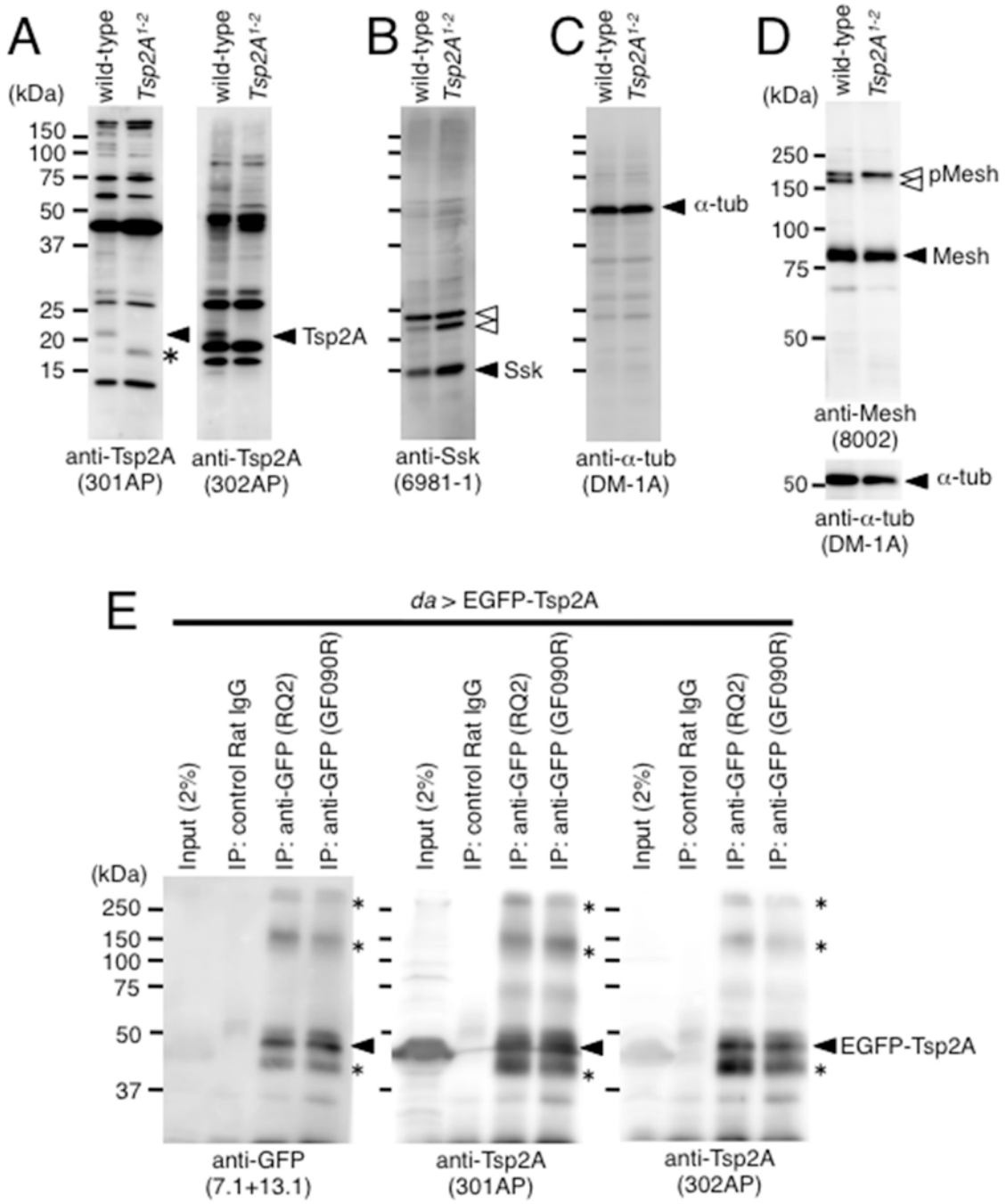

Figure S3. Anti-Tsp2A antibodies recognize endogenous and exogenous Tsp2A in Western blots.

(**A-C**) Extracts of the first-instar larva prepared from wild-type *Drosophila* and *Tsp2A*$^{1-2}$-mutants were separated on a 15% SDS-polyacrylamide gel, and Western blot analyses were performed using anti-Tsp2A (A, left panel, 301AP; right panel, 302AP), anti-Ssk (B) and anti-α-tubulin (C) antibodies. A protein band of ~21 kDa was detected by anti-Tsp2A antibodies in the wild-type but not in the *Tsp2A*$^{1-2}$-mutant (A; arrowheads), suggesting that the ~21 kDa band represents Tsp2A. Instead, an ~18 kDa band was detected by anti-Tsp2A antibody (301) in the *Tsp2A*$^{1-2}$-mutant extract (A; asterisk of left panel). Protein bands other than the ~21 kDa band, detected by each

anti-Tsp2A antibody seem to originate from cross-reactions because they are observed in both of wild-type and *Tsp2A*$^{1\text{-}2}$-mutant larvae (A). The density of the main band of Ssk (~15 kDa) is not significantly different in the *Tsp2A*$^{1\text{-}2}$-mutant relative to the wild-type (B; arrowhead). White arrowheads in B indicate non-specific bands detected by anti-Ssk antibody. Western blots using anti-α-tubulin antibody show that the same quantities of protein were loaded in the wild-type and *Tsp2A*$^{1\text{-}2}$-mutant extracts (C).

(D) Extracts of first-instar larvae prepared from wild-type *Drosophila* and the *Tsp2A*$^{1\text{-}2}$-mutant were separated on an 8% SDS-polyacrylamide gel and Western blot analyses were performed using anti-Mesh (D; upper panel), and anti-α-tubulin (D; lower panel) antibodies. The density of the main band of Mesh is not significantly different in the *Tsp2A*$^{1\text{-}2}$-mutant compared with the wild-type (D; arrowhead). However, the higher-molecular-mass band of Mesh is visible as a double band at ~200 kDa in the wild-type (upper and lower white arrowhead) but as a single band in the *Tsp2A*$^{1\text{-}2}$-mutant (upper white arrowhead). Western blots using anti-α-tubulin antibody show that the same quantities of protein were loaded in the wild-type and *Tsp2A*$^{1\text{-}2}$-mutant extracts (lower panel).

(**E**) The extracts of embryos expressing EGFP-Tsp2A with the *da*-GAL4 driver (Input) were subjected to immunoprecipitation (IP) with rat IgG and two kinds of anti-GFP antibodies (RQ2 or GF090R). The immunocomplexes were separated on a 12% SDS-polyacrylamide gel and Western blot analyses were performed using anti-GFP antibody (left panel) or anti-Tsp2A antibody (301AP; middle panel or 302AP; right panel). In addition to the main band of EGFP-Tsp2A (arrowhead), weak bands at 250, 150, and 40 kDa are detected by these antibodies (asterisks). In the input lanes, the specific bands of EGFP-Tsp2A were undetectable by these antibodies.

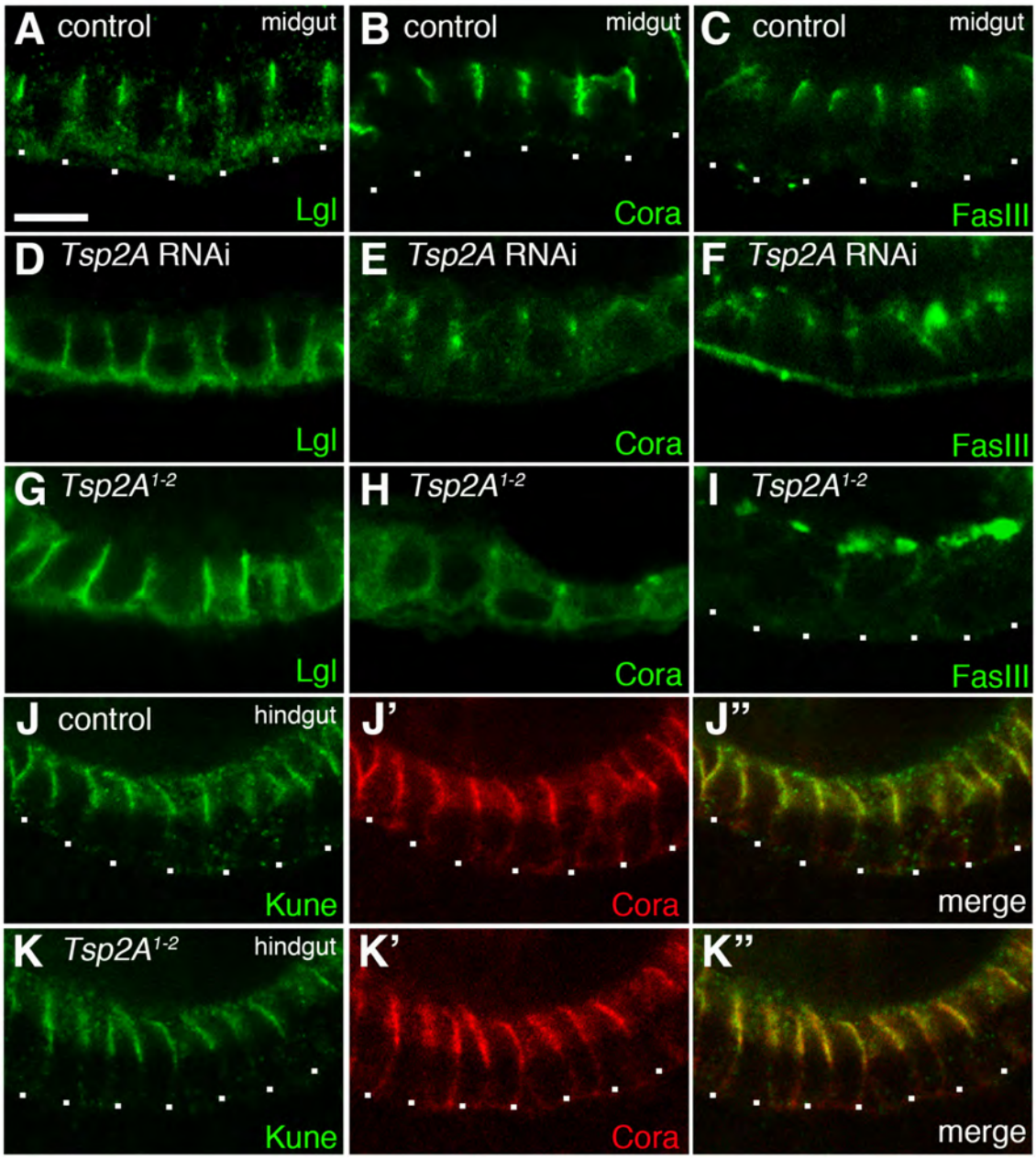

Figure S4. A *Tsp2A* mutation causes mislocalization of SJ components in the midgut.

(**A-I**) The first-instar larval OELP of control (A-C), *Tsp2A*-RNAi 11415R-2 (D-F) and $Tsp2A^{1-2}$-mutant (G-I) stained with anti-Lgl (A, D and G), anti-Cora (B, E and H) and anti-FasIII (C, F and I) antibodies.

(**J-K"**) Antibody double-staining of stage-16 control (J-J") and $Tsp2A^{1-2}$-mutant (K-K") embryos using anti-Kune (J and K) and anti-Cora (J' and K') antibodies. The merged images are shown in J" and K". Basal membranes are delineated by dots. Scale bar: 5 µm.